

# Monitoring of riparian vegetation response to flood disturbances using terrestrial photography

Katarina Dzubakova<sup>1,2</sup>, Peter Molnar<sup>1</sup>, Konrad Schindler<sup>3</sup>, and Milan Trizna<sup>2</sup>

<sup>1</sup>Institute of Environmental Engineering, ETH Zurich, Switzerland

<sup>2</sup>Department of Physical Geography and Geoecology, Comenius University in Bratislava, Slovakia

<sup>3</sup>Institute of Geodesy and Photogrammetry, ETH Zurich, Switzerland

*Correspondence to:* Peter Molnar  
(molnar@ifu.baug.ethz.ch)

**Abstract.** Riparian vegetation on river floodplains is significantly impacted by floods. In this study we use a high resolution ground-based camera system with near-infrared sensitivity to quantify the immediate response of riparian vegetation in an Alpine gravel bed braided river to flood disturbance with the use of vegetation indices. Five largest floods with return periods between 1.4 and 20.1 years in the period 2008–2011 in the Maggia River were analysed to evaluate patterns of vegetation response in three distinct floodplain units (main bar, secondary bar, transitional zone) and to compare the sensitivity of seven vegetation indices. The results show both negative (damage) and positive (enhancement) response of vegetation in a short period following floods, with a selective impact based on the geomorphological setting and the intensity of the flood forcing. The spatial distribution of vegetation damage provides a coherent picture of floodplain response in the three floodplain units. We show that the tested vegetation indices generally agree on the direction of predicted change and its spatial distribution. The disagreement between indices was in the range 14.4–24.9% despite the complex environment, i.e. highly variable surface wetness, high gravel reflectance, extensive water-soil-vegetation contact zones. We conclude that immediate vegetation response to flood disturbance may be effectively monitored by terrestrial photography with near-infrared sensitivity, with potential for long-term assessment in river management and restoration projects.

with floodplains and river marginal wetlands provides a range of important ecosystem services such as biodiversity, flood retention, nutrient sink, pollution control, groundwater recharge, carbon sequestration, timber and organic matter production, and recreation (e.g. Tockner et al., 2008). The species composition and spatial distribution of riparian vegetation is largely determined by the floodplain morphology and the river flow regime (e.g. Bendix and Hupp, 2000; Merritt et al., 2010; Gurnell et al., 2012) as well as by plant tolerance and response to flood disturbance and water stress (e.g. Auble et al., 1994; Blanch et al., 1999; Glenz et al., 2006; Pasquale et al., 2012). The reciprocal interactions between hydromorphological processes and riparian vegetation lead on the long term to the formation of complex mosaics of landforms and their respective biological communities and habitat patches (e.g. Pringle et al., 1988; Gregory et al., 1991; Decamps, 1996; Latterell et al., 2006; Gurnell and Petts, 2006; Corenblit et al., 2007; Gurnell and Petts, 2011).

The flood impact on riparian vegetation is well documented. The most apparent is a direct negative impact when the vegetation is scoured (Bendix, 1999; Edmaier et al., 2011; Crouzy et al., 2013), covered by sediment and debris (Ballesteros et al., 2011), drowned (Friedman and Auble, 1999), or loses connection to the water table due to channel displacement (Loheide and Booth, 2011). A less evident negative impact of floods is a general decrease in vegetation vigor associated with the post-stress reaction of plants. Plants under flood-induced stress have both short-term and long-term physiological and morphological responses (Kozłowski and Pallardy, 2002), such as decreased photosynthetic activity, plant growth, dry matter production, reproduction, and root mortality (e.g. Hatfield, 1997; Toda et al., 2005). On the other hand, floods can positively influence riparian vegeta-

## 1 Introduction

Riparian vegetation is under natural conditions a dynamic component of the riverine environment, which together

tion by the generation of new germination sites and the distribution of propagules and woody debris (Gurnell and Petts, 2006; Bertoldi et al., 2011a; Gurnell et al., 2012), and by enabling access to water and nutrients in previously disconnected parts of the floodplain (Amoros and Bornette, 2002).

Some of these relationships have been replicated in flume experiments (e.g. Tal and Paola, 2010; Perona et al., 2012) and used in numerical modelling (e.g. Perona et al., 2009a,b).

The monitoring of riparian vegetation in floodplains can be achieved by a range of sensors and methods (see review in Carbonneau and Piégay (2012)). Changes in riparian vegetation cover at the large scale are commonly quantified with remotely sensed data, such as satellite imagery (Verrelst et al., 2008; Johansen et al., 2010; Bertoldi et al., 2011a,b; Caruso et al., 2013; Parsons and Thoms, 2013) and aerial photography (e.g. Bertoldi et al., 2011a,b; Mulla, 2012). These are usually suitable for applications to large rivers at irregular time sampling. More recently, Unmanned Aerial Vehicles (UAVs) (e.g. kites, helicopters, planes, paragliders) have been used for monitoring with high resolution and large data coverage, at a sampling rate determined by the operator (Berni et al., 2009; Dunford et al., 2009; Zhang and Kovacs, 2012).

A complementary approach for detailed local analysis of riparian vegetation activity at the scale of individual gravel bars is terrestrial photography. Similarly to UAV systems, terrestrial photography has the advantage of a high spatial resolution ( $< 10^0$  m) and a user-defined regular high time sampling rate. In addition, terrestrial photography by fully automatic systems has practically no running costs after installation. Disadvantages are a restricted areal coverage and limits of oblique photography (e.g. Morgan et al., 2010; Crouzy et al., 2013). Since one of our main goals is to quantify short-term floodplain response to floods we have opted for terrestrial monitoring by cameras, where we can obtain images shortly before and immediately after large flood events. Our photographic monitoring system is focused on a gravel bar where the recorded imagery in the visible and near-infrared range is processed into several broadband vegetation indices.

Vegetation indices (VIs) capture properties of leaf surface pigmentation, photosynthetic activity and canopy structure. Many VIs exist in the literature, each with their own advantages and disadvantages. The choice of a suitable vegetation index depends on plant specifics (Bargain et al., 2013), the environment (Barati et al., 2011), the target plant property or attribute (Ortiz et al., 2011; Sims and Gamon, 2003), and availability of spectral bands (Adam et al., 2010). The ratio vegetation index (RVI) and green RVI (GRVI) are the simplest conventional VIs, the normalized difference vegetation index (NDVI) and green NDVI (GNDVI) belong to differential indices. Both, RVI and NDVI are sensitive to optical properties of the soil background (Baret et al., 1991). Their sensitivity is even more pronounced with increasing sparseness of the vegetation cover (Eckert and Engesser, 2013)

which is specific for riparian systems. To reduce the impact of soil reflectance, different modifications of the soil-adjusted vegetation index (SAVI) were developed (Huete, 1988; Baret et al., 1991; Qi et al., 1994). Other indices, such as the chlorophyll vegetation index (CVI), focus on the green band reflectance of plants (Ortiz et al., 2011). In this study we have used a selection of these most common broadband indexes (Table 1). We cannot use narrowband vegetation indices which are better predictors of leaf pigment content (e.g. Sims and Gamon, 2002; Berni et al., 2009; Zarco-Tejada et al., 2009), but require reflectance measurements with a high spectral frequency resolution, which cameras do not provide.

The main aims of this study are: (1) to analyze the spatial distribution and intensity of the vegetation response to large floods, where we aim to capture not only severe vegetation damage and erosion, but also the less apparent change of vegetation vigor; (2) to study the vegetation response in three distinct floodplain units of a gravel bar (main bar, secondary bar, transitional zone) which are meaningful units with regard to the concept of the floodplain mosaic system; and (3) to provide the results for several vegetation indices to study their agreement in identifying the direction and magnitude of floodplain change. The analysis was performed for five floods in a four year period (2008–2011) on a gravel bar of an Alpine braided river (Maggia River, Switzerland). The relatively numerous flood events within the four study years enabled us to assess the vegetation response of the same species composition to different flood stages and longer term weather conditions.

## 2 Study Area

Maggia is an Alpine river located in southeast Switzerland, north of the city of Locarno. The river originates at an altitude of about 2500 m and flows south through the Maggia Valley into Lake Maggiore (193 m). The bedrock of the valley is formed by Penninic Crystalline Nappe predominantly covered by Holocene alluvial deposits. Within these settings Maggia evolved into a braided river system with a gravel cobble bed occasionally covered with fine sediment deposits on elevated alluvial bars. The average bed slope in the main valley is about 0.8%.

The hydrological regime of the river is significantly influenced by hydropower infrastructure (dams, intakes, canals) constructed in the upper watershed in the 1950s. Since then, approximately 75% of the natural river flow has been diverted to the power station Verbano at Lake Maggiore and only minimum flows are released into the main valley. At present, the bypassed section has an average daily streamflow of  $4.1 \text{ m}^3\text{s}^{-1}$ , while it was close to  $16 \text{ m}^3\text{s}^{-1}$  prior to 1954 (Molnar et al., 2008). The 100-year flood peak is estimated at  $768 \text{ m}^3\text{s}^{-1}$  (Bignasco) at the upper end of our study reach. The hydropower system regulation practically

removes the snowmelt spring-summer flow peak in the valley, but does not affect the largest floods appreciably, mainly due to the upstream location of reservoirs and their relatively low storage capacity. As a consequence, floods with a perceptible impact on riparian vegetation still occur on the average more than once per year in the main valley (Perona et al., 2009a).

In this study we focused on the 500 m long and 300–400 m wide reach of the river in the main valley located between the villages Someo and Giumaglio. Three distinct floodplain units were identified within the study reach, namely main gravel bar (MB), secondary gravel bar (SB), and a transitional zone (TZ) (Fig. 1). The main bar is the largest, most elevated unit. It is located in the center of the floodplain in close proximity to the main channel. The secondary bar is at the edge of the floodplain. Both bars are separated by a transitional zone with very active channel dynamics. The secondary channel in the transitional zone is fully connected with the main channel only during the largest flood events.

The vegetation composition within the study reach is heterogeneous (Fig. 2). The dominant willows (salix species) are *Salix purpurea*, *Salix alba*, *Salix eleagnos*, often accompanied by poplars (*Populus nigra*) and alders (*Alnus incana*), occasionally by maples (*Acer pseudoplatanus*), lindens (*Tilia cordata*), fallopias (*Fallopia sachalinensis*), and locusts (*Robinia pseudoacacia*). The tree height varies from 1 to 10 m. Sparse herbaceous cover grows sporadically on the inner part of the bars with sand accumulation. The variability in the vegetation composition within the three studied floodplain units is notable. *Salix* individuals are located at the upstream part of MB, and towards its inner part are often accompanied by poplars. Unlike on MB, *salix* is predominantly mixed with *fallopia* on SB. Although fewer in number, the largest diversity in species is found in TZ with *Alnus*, *Salix*, locally *Populus* and *Acer*.

### 3 Data and Methods

#### 3.1 Meteorological and hydrological data

Hourly records of solar radiation, air temperature, relative humidity, and rainfall used in this study were obtained from the weather station Locarno-Monti (MeteoSwiss), located about 15 km downstream from the study reach. Hourly streamflow is gauged on the Maggia River at Bignasco (FOEN) approximately 7.8 km upstream of the study reach. There is an ungauged small tributary (Rovana) between the gauging station and our study reach, thus the peak flows of the studied floods in our reach are a lower estimate.

We analysed the five largest summer floods in the period 2008–2011 with return periods between 1.4 and 20.1 years (Table 2). The upstream part of the MB and the TZ were submerged during all studied floods, the SB and central part of the MB were submerged only in 2011. We defined

the duration of the floods based on the discharge exceeding  $180 \text{ m}^3 \text{ s}^{-1}$ . This corresponds approximately to the discharge when the river inundates the majority of the riparian zone. For lesser discharges the vegetation damage by scour is minimal. The flood peaks of the first four floods reached a discharge of  $180 \text{ m}^3 \text{ s}^{-1}$  once for several hours thus they are considered to be single-peak floods. The flood in 2011 consisted of two flood peaks greater than  $180 \text{ m}^3 \text{ s}^{-1}$  over a period of five days.

The meteorological conditions and streamflow before and after each flood are summarized in Fig. 3. The flood in May 2008 was the earliest in the season with the lowest air temperature (minimum  $10^\circ \text{C}$ ) and the highest relative humidity prior to the event. The raingauge at Locarno-Monti did not capture the storm rainfall which occurred mostly in the headwaters of the catchment. With the flood peak of  $192 \text{ m}^3 \text{ s}^{-1}$ , it was the smallest but at the same time the longest flood analysed. There were two floods with similar peaks in 2009. The summer of 2009 was very dry and hot, air temperatures prior to both floods reached or exceeded  $30^\circ \text{C}$ , relative humidity was generally very low. The flood in June had intense rainfall ( $40 \text{ mm h}^{-1}$ ) measured in Locarno-Monti and the flood peak reached  $254 \text{ m}^3 \text{ s}^{-1}$ . The subsequent flood in July was preceded by three days of moderately intense rainfall ( $20 \text{ mm h}^{-1}$ ) and reached a flood peak of  $272 \text{ m}^3 \text{ s}^{-1}$ . The flood in June 2010 occurred during a period with average air temperature around  $20^\circ \text{C}$  and high relative humidity. With the flow reaching  $301 \text{ m}^3 \text{ s}^{-1}$  it was the second largest analysed flood. The raingauge in Locarno-Monti captured the storm event only partially, while heaviest precipitation occurred in the upper catchment. The largest flood in June 2011 also occurred during a period with average air temperature slightly above  $20^\circ \text{C}$ . Intense rainfall covered the entire basin and was measured at Locarno-Monti with intensities about  $40 \text{ mm h}^{-1}$  for a short duration. The flood peak reached  $598 \text{ m}^3 \text{ s}^{-1}$ .

#### 3.2 Image collection and processing

The camera installation in the Maggia River consists of two digital cameras (Canon EOS 350D, 24 mm lens and 8 Mpx CCD sensor). The two cameras are placed next to each other in a weather-proof box. The box is placed on a steep rocky ridge above the river to give an unobstructed view of the floodplain at the highest angle we could safely get to. The depression angle to the center of the image on the floodplain is  $25^\circ$ , the horizontal distance to the study reach is between 860 and 1460 m, the vertical distance is 537 m. The camera box is accessible only by foot, along a steep mountain path. Photographs are triggered with a Timer Remote Control every 24 hrs at 11:00 UTC from summer 2008. The images are stored locally in the cameras on CF memory cards. The cameras are powered by Canon Li-Ion 700 mAh batteries. We visit the camera location 3 times a year to replace batteries, download the images, and perform basic maintenance (cleaning).

The first camera is a regular camera recording the R-G-B visual bands. The second camera is adjusted to be sensitive in the near-infrared range (780-900 nm) by replacing the UV/IR blocking filter on the sensor with a clear filter and a 780 nm IR filter on the lens (heliopan IR780). Sample images can be seen in Fig. 1B. Unlike studies which use cameras with automatic settings or webcams (e.g. Richardson et al., 2007, 2009; Mizunuma et al., 2011), we fixed all adjustable settings manually (except white balance) so that we can directly compare the digital numbers DN<sub>s</sub> (brightness at sensor) in the RGB bands and the NIR band in all images without transformations.

To fix the key camera settings (focus, aperture, exposure) to the best average lightning conditions in the valley we looked at the image DN<sub>s</sub> of the floodplain in the R-NIR space for a range of typical light conditions. We explored the aperture and time setting ranges to make sure that even for the brightest days we had only limited saturation of pixels in both bands (over-exposure). This analysis led us to fix the aperture on both cameras to  $f=11$  and the exposure time to 1/160 s for the RGB camera and 1/40 s for the NIR camera. Images with significant light limitations were discarded based on their RGB histograms below set thresholds. These were images with usually very low visibility on rainy days or presence of haze/mist or low lying cloud cover, and VIs computed on them would contain large uncertainty.

The image processing required several steps. Firstly the images were converted to TIFF 48-bit format and registered using a cross-correlation algorithm which searches for the shift in horizontal and vertical directions to obtain the best pixel-based fit. Images with significant light limitations due to haze or high relative humidity were automatically identified based on their color histograms and excluded from further analysis. Seven VIs (Table 1) were computed on the registered images and the VI images were subsequently orthorectified. The image resolution after orthorectification was 0.5 m, therefore individual shrubs and trees on the gravel bar are easily visible. The images capture the herbaceous cover only occasionally due to its sparse distribution and its growth on the sand accumulations close to the higher vegetation.

In order to link the DEM and field observations as well as to obtain the real proportion of vegetation cover, two orthorectification methods were tested. While planar orthorectification defined by five rectification points of distinct fluvial features resulted in an evenly distributed image distortion of 1-2 pixels ( $< 1\text{m}$ ), the orthorectification based on a LiDAR DEM (2 m resolution) was better in areas with reliable LiDAR points but significantly distorted ( $\sim 2.5\text{ m}$ ) in zones with decreased LiDAR DEM accuracy. Since our study reach is indeed a very flat surface, we decided to apply planar orthorectification in our analysis. The image distortion is acceptable for studying individual riparian trees and patches which have footprints much greater than 1 m.

### 3.3 Vegetation index analysis

The flood impact on riparian vegetation was evaluated by comparison of VIs from a period before and after each flood event. To obtain a statistically robust measure of the vegetation activity, given the variability between days in terms of light conditions following a storm, we defined the before-flood  $VI^{bf}(t)$  and post-flood  $VI^{pf}(t)$  arrays as

$$VI^{bf}(t) = \text{median}(VI(t-k); k = 1, \dots, 7), \quad (1)$$

$$VI^{pf}(t) = \text{median}(VI(t+k); k = 1, \dots, 7), \quad (2)$$

where  $VI(t)$  is the vegetation index value on day  $t$  and the median is computed pixel-wise. We chose the median VI pixel value for a period  $k$  before and after each flood in order to reduce the potential impact of adverse light conditions and shadows on the images in individual days. We experimented with different  $k$  values and found that  $k = 7$  days provided an acceptable smoothing without destroying the signal in the data. Although the images after a flood peak may be affected by the flood recession, most studied floods had recessions less than 24 hrs long, so this effect is not likely to persist for more than 1-2 days (images) and these will not affect the pixel-based median of the estimated vegetation change.

We then computed the difference between the two arrays to get the vegetation change array

$$\Delta VI(t) = VI^{pf}(t) - VI^{bf}(t). \quad (3)$$

Negative values of  $\Delta VI$  indicate a decrease in the vegetation index after the flood, e.g. by the erosion and damage of vegetation, while positive values indicate an increase in the vegetation index after the flood, e.g. rise in photosynthetic activity and growth. To analyze vegetation change we selected only pixels representing vegetation cover prior to the flood (i.e.  $VI^{bf} > 0.15$ ) for further processing.

To compare the indices we took the vegetation change array for each flood for a pair of indices  $\Delta VI_1$  and  $\Delta VI_2$ , and we estimated an index of disagreement as

$$ID(t)_{1,2} = \text{area}(\Delta VI_1(t) \cdot \Delta VI_2(t) < 0) / \text{total area}. \quad (4)$$

The index of disagreement ID between all floods was averaged and is reported in Table 3 for all VI index pairs. In presenting the results we used the index that gives on the average the lowest disagreement with all the other indices in terms of the direction of predicted vegetation change, i.e. overall vegetation damage ( $\Delta VI < 0$ ) and enhancement ( $\Delta VI > 0$ ). It should be noted that our intent is not to select the single best vegetation index, rather we want to compare the differences in the performance of several vegetation indices all of which have been validated in the literature. Ground validation by spectroradiometry in the field is planned in the future. Our assumption is that all analyzed VIs reliably represent vegetation activity and that the differences among the indices will occur mainly on the water-soil-vegetation contact zones due

to their different sensitivities. The sensitivity of the VIs to captures vegetation scour within our study reach is shown in Fig. 4, for the largest flood in 2011.

## 4 Results

### 4.1 Comparison of vegetation indices

To quantify the vegetation response to floods we first report the overall comparison of the VIs by the index of disagreement in Table 3. The results show that the chosen VIs capture the trends of vegetation response (i.e. vegetation damage or enhancement) coherently, as the pair-wise differences of the indices vary between 0.7 and 32.2%. Generally, the indices based on the same visible band tend to show more similar results in comparison to indices based on different visible bands. The RVI and GRVI differ by only 0.7% from their normalized derivatives NDVI and GNDVI, and by 10.1–12.3% from the soil-adjusted derivatives SAVI and GSAVI. On average, GNDVI (14.4 %), GRVI (14.5 %), NDVI (16.8 %), and RVI (16.8 %) have the lowest disagreement with the other indices, while CVI (24.9 %) differs the most.

### 4.2 Vegetation response in time

Vegetation response measured by  $\Delta VI$  conditioned on the pre-flood vegetation vigor and river morphology gives us the most complete picture of the nature of flood-induced vegetation change. In Fig. 5 we show the boxplots of  $\Delta VI$  as a function of the pre-flood  $VI^{bf}$  for the three floodplain units and five floods using the GNDVI. Only pixels with vegetation cover prior to the flood, i.e.  $VI^{bf} > 0.15$  are considered in the analysis.

The first result comes from the statistical distribution of  $VI^{bf}$  for the floodplain units which shows that most vegetation is growing on the main bar, considerably less on the secondary bar and in the transitional zone. All three floodplain units exhibit modes at  $VI^{bf} = 0.3 - 0.4$ , which correspond to healthy and large individual plants. Vegetation with  $VI^{bf} = 0.4 - 0.5$ , i.e. the highest computed VI, is present in all three floodplain units, especially in the transitional zone. Comparing the pre-flood vegetation conditions for the period 2008–2011, the vegetation composition appears to be reasonably stable, there is limited evidence for widespread scouring or vegetation growth in all three floodplain units at this temporal scale. Scouring of a small extent is visible between the flood in 2008 and 2009.

The second result is the detailed effect of the individual floods. Riparian vegetation tends to be both damaged and enhanced after each flood at the floodplain unit scale. Vegetation with lower  $VI^{bf}$  responds to flood disturbance with greater absolute change for the smaller floods. At the same time, while vegetation damage occurs for all  $VI^{bf}$  categories, vegetation enhancement is more likely to occur for vegetation with higher  $VI^{bf}$ , i.e. stronger and larger plants. This

indicates a selective destructive effect on smaller or weaker plants and enhancement for stronger individuals.

Perhaps most striking is the difference between the intensity of vegetation response to the first four smaller floods and to the largest flood in July 2011. The first four floods show on average rather small changes, while the flood in 2011 shows considerably greater impact on vegetation, changes as high as  $\Delta VI = -0.4$  were found indicating complete removal of plants. These erosive effects have however not affected the strongest plants, in fact the areas with highest pre-flood  $VI^{bf}$  have experienced an enhancement of the VI index in the week following the flood, especially on the main bar.

### 4.3 Spatial distribution of vegetation response

The intensity of the vegetation response to floods differs between the floodplain units. The main bar has moderate response with  $\Delta VI$  mostly between -0.1 and 0.1 (outliers excluded) for the first four floods and between -0.2 and 0.15 for the flood in 2011. The secondary bar has slightly smaller vegetation response than the vegetation on the main bar. The exception is the response after the flood in 2011, where significant damage is evident for low  $VI^{bf}$ . Unlike the vegetation response on the bars, the  $\Delta VI$  range in the transitional zone fluctuates considerably more, from -0.2 to 0.15 for the first four floods, and from -0.4 to 0.2 for the flood in 2011. The transitional zone is an area of flow divergence and channel shifting during large floods.

The spatial distribution of  $\Delta VI$  is shown in Fig. 6. The area with the most negatively affected vegetation appears to be the transitional zone and the contact zone between the main bar and the river. On the other hand, vegetation enhancement is characteristic for the central parts of the main bar.

The flood in May 2008 with its long duration early in the vegetation season caused a similar intensity but a slightly different spatial distribution of vegetation response compared to the following floods. The different vegetation response might have also been impacted by the presence of plants in close proximity to the main channel and on the top of the transitional zone that were scoured in autumn 2008. Particularly interesting is the impact of the shortest analysed flood in July 2009 that occurred only one month after the flood in June 2009. It was the only flood with widespread vegetation enhancement, most likely associated with surface water supply to the floodplain. The largest flood in 2011 is the only analysed flood which caused severe vegetation damage, local scour, mostly on the upper part of the main alluvial bar and in the transitional zone. Despite the predominantly destructive impact of this flood by scour (see also Fig. 4), the inner most elevated parts of the main bar also show significant vegetation enhancement, probably caused by wetting of the inundated surfaces.

## 5 Discussion

Terrestrial photography is a viable approach for the continuous monitoring of riparian vegetation as attested by emerging recent studies (e.g. Richardson et al., 2009; Bertoldi et al., 2011b; Mizunuma et al., 2011; Welber et al., 2012; Crouzy et al., 2013; Pasquale et al., 2014). We consider such monitoring to be a valuable low-cost alternative for continuous repeated measurement and analysis of change in riverine environments which are considered worldwide to be among the most threatened ecosystems (Nilsson and Berggren, 2000; Tockner and Stanford, 2002). The application of VIs in our study to analyze change after floods raised some questions connected to the peculiarities of the riverine environment.

The VIs were estimated for a heterogeneous and highly dynamic riverine environment characterized by a variable surface wetness, high gravel reflectance, extensive water-soil-vegetation contact zones, and riparian vegetation with different density and reflectance properties. This is a very challenging environment compared to usual settings in published literature on camera monitoring of vegetation, where a particular species or canopies are being studied in isolation (e.g. Ahrends et al., 2008; Richardson et al., 2009; Mizunuma et al., 2011; Nagai et al., 2012) or in homogeneous soil substrate with relatively low reflectance (e.g. Viña et al., 2011; Mulla, 2012). The complexity of the environment is reflected in the variability of the estimated vegetation response by the different indices (disagreement between 14.4–24.9% on average). On the other hand, the spatial prediction of change shows substantial coherence (see Fig. 6) even for the largest flood in 2011, which is a promising result for applications in riparian environments.

The differences between VIs have been addressed in the literature (e.g. Jackson and Huete, 1991; Glenn et al., 2008). In the riverine environment, our selected indices using the same visible band tended to have noticeably more similar results than the indices based on different visible bands. We attribute this tendency to the fact that the red visible band is more sensitive to chlorophyll in healthy leaves, while the green visible band is more sensitive to chlorophyll in weakened leaves (Gitelson et al., 1996). Thus, we presume that the indices based on different visible and near-infrared bands will have different sensitivities which will be plant and season specific. Overall, we conclude that although all studied vegetation indices did appear to capture essential information on vegetation change coherently, future work should be directed at the validation of index performance in the riverine environment (e.g. Parsons and Thoms, 2013), in order to better understand local effects of soil-sediment reflectance, vegetation type, height, and sparseness.

Considering the general trend of vegetation response, prevailing damage of vegetation with low  $VI^{bf}$  and enhancement of vegetation with high  $VI^{bf}$  by floods indicate connections between vegetation stability, growth, and vigor. Smaller plants, predominantly *Salix* individuals, on surfaces exposed

to more frequent and damaging stress during floods have a harder time to recover between floods (Perona et al., 2012), while more protected locations on the gravel bar and floodplain provide a better environment for plants to germinate and grow (zones generally populated by *Salix*, *Populus*, occasionally by *Alnus*, *Tilia*, or *Acer*). This supports the spatial distribution of riparian vegetation within the floodplain (Gurnell et al., 2012). Increasing vegetation diversity in close proximity to the secondary channel in the transitional zone indicates the existence of lateral flow from the channel, and perhaps also less suitable habitat conditions in the middle of the bars. Additional complexity is added to this picture by the sediment structure. The presence of fine material in the substrate and a coarse gravel layer on the surface inhibiting evaporation have been shown to be critical for maintaining a high soil moisture after inundation (Meier and Hauer, 2010) and will likely impact the degree of vegetation enhancement following floods.

The floodplain units displayed different vegetation composition and response to floods. The main bar, populated by *Salix* and *Populus* individuals, was the most vegetated area with the most variable spatial pattern of vegetation response to flood disturbances. The *Salix* and *Fallopia* individuals on the secondary bar had generally lower index values than the vegetation on the main bar despite the fact that it is flooded less often than the vegetation on the main bar. The transitional zone was found to be the zone with the most diverse composition (*Salix*, *Alnus*, *Populus*, and others), but at the same time the most sensitive vegetation to floods, especially due to lateral erosion of the secondary channel (observed during the field campaign). The results are in accord with the understanding of the floodplain as a mosaic system, where each floodplain unit is determined by its specific morphological, hydrological, and biotic site conditions (Bendix and Hupp, 2000; Jacobson, 2013). More importantly, our study suggests that the mosaic system perspective on vegetation response is perhaps not only valid in a long-term perspective as shown in previous literature, but also on short flood response time scales.

## 6 Conclusions

This study demonstrated the use of a high resolution ground-based infrared-sensitive camera monitoring of riparian vegetation in an Alpine gravel bed braided river. The focus was on quantifying the immediate response of riparian vegetation to flood disturbance by standard vegetation indices.

The results offer new insights into the complexity of riparian vegetation dynamics within a floodplain. The main results from a study of five largest floods with return periods between 1.4 and 20.1 years in the period 2008–2011 on a reach in the gravel bed braided Maggia River in Switzerland were: (1) Riparian vegetation displays both negative (damage) and positive (enhancement) response in a short pe-

riod after floods. There is evidence for a selective impact based on the morphological setting and flood forcing, with destructive effects on smaller or weaker plants and enhance-  
 590 In general, the most impacted plants are young *Salix* individuals on the upstream part of the floodplain, as well as considerably older vegetation (*Salix*, *Populus*, and *Alnus*) in close proximity to the secondary channel where lateral erosion takes place. (2) The intensity and spatial distribution of  
 595 vegetation damage provides a coherent picture of the floodplain response in three distinct units (main bar, secondary bar, transitional zone) with different inundation potential and flood stress. A threshold effect is apparent, with the largest  
 600 flood in 2011 producing by far the greatest change. (3) We demonstrated that standard vegetation indices provide means to quantify vegetation response even in this heterogeneous environment characterized by a mixture of gravel and water  
 605 surfaces and riparian vegetation with different density and reflectance properties. The seven tested indices agreed on the direction of change and its spatial distribution despite many site specifics, e.g. variable surface wetness, high gravel reflectance, and extensive water-soil-vegetation contact zones, with a disagreement on the average between 14.4 and 24.9%.

One of the main aims of this paper was to provide an analysis of a ground-based infrared-sensitive camera monitoring  
 610 setup which provides high spatial and temporal resolution of riparian vegetation change at a gravel bar and river reach scale. The resolution provides a considerable advantage over remote sensing by satellites with the downside connected to  
 615 the broadband nature of the reflectance data. A practical advantage of such a system is the low purchasing and maintenance cost. We are convinced that such systems are suitable for long-term monitoring of riparian areas and have high potential for river management, particularly for regulated rivers  
 620 or rivers with restoration projects.

**Acknowledgements.** This research was funded by the Scientific Exchange Program Sciex-NMS Grant 12.111, the Slovak Research and Development Agency Grant APVV-0625-11, and the Slovak Scientific Grant Agency VEGA Project 1/0937/11. Meteorological data  
 625 was provided by MeteoSwiss (Federal Office of Meteorology and Climatology). Hydrological data were provided by FOEN (Federal Office for the Environment). We thank Ondrej Budac (EPFL, Switzerland) for his technical support. We are grateful for comments and questions raised by three anonymous reviewers which  
 630 significantly improved our work.

## References

Adam, E., Mutanga, O., and Rugege, D.: Multispectral and hyperspectral remote sensing for identification and mapping of wetland vegetation: a review. *Wetlands Ecology and Management*, 18(3), 281–296, 2010.  
 635  
 Ahrends, H.E., Bruegger, R., Stoeckli, R., Schenk, J., Michna, P., Jeanneret, F., Wanner, H., and Eugster, W.: Quantitative phenological observations of a mixed beech forest in northern Switzerland with digital photography, *J. Geophys. Res.*, 113, 2008.

Auble, G. T., Friedman, J. M., and Scott, M. L.: Relating riparian vegetation to present and future streamflows, *Ecol. Appl.*, 4(3), 544–554, 1994.  
 Amoros, C. and Bornette, G.: Connectivity and biocomplexity in waterbodies of riverine floodplains, *Freshwater Biology*, 47(7), 761–776, 2002.  
 Ballesteros, J. A., Bodoque, J. M., Diez-Herrero, A., Sanchez-Silva, M., and Stoffel, M.: Calibration of floodplain roughness and estimation of flood discharge based on tree-ring evidence and hydraulic modelling, *J. Hydrol.*, 403(1–2), 103–115, 2011.  
 Barati, S., Rayegani, B., Saati, M., Sharifi, A., and Nasri, M.: Comparison the accuracies of different spectral indices for estimation of vegetation cover fraction in sparse vegetated areas, *The Egyptian Journal of Remote Sensing and Space Science*, 14(1), 49–56, 2011.  
 Baret, F., Guyot, G., and Major, D. J.: TSAVI: a vegetation index which minimizes soil brightness effects on LAI and APAR estimation, in *Proceedings of the 12th Canadian symposium on remote sensing and IGARSS*, Vancouver, Canada, 1355–1358, 1991.  
 Bargain, A., Robin, M., Méléder, V., Rosa, P., Le Menn, E., Harin, N., and Barillé, L.: Seasonal spectral variation of *Zostera noltii* and its influence on pigment-based Vegetation Indices, *J. Experimental Marine Biology and Ecology*, 446, 86–94, 2013.  
 Bendix, J.: Stream power influence on southern Californian riparian vegetation, *J. Vegetation Sci.*, 10, 243–252, 1999.  
 Bendix, J. and Hupp, C. R.: Hydrological and geomorphological impacts on riparian plant communities, *Hydrol. Process.*, 14, 2977–2990, 2000.  
 Berni, J., Zarco-Tejada P. J., Suarez, L., and Fereres, E.: Thermal and Narrowband Multispectral Remote Sensing for Vegetation Monitoring From an Unmanned Aerial Vehicle, *IEEE Transactions on Geoscience and Remote Sensing*, 47(3), 722–738, doi:10.1109/TGRS.2008.2010457, 2009.  
 Bertoldi, W., Drake, N. A., and Gurnell, A. M.: Interactions between river flows and colonizing vegetation on a braided river: exploring spatial and temporal dynamics in riparian vegetation cover using satellite data, *Earth Surf. Process. and Landforms*, 36(11), 1474–1486, 2011a.  
 Bertoldi, W., Gurnell, A. M., and Drake, N. A.: The topographic signature of vegetation development along a braided river: Results of a combined analysis of airborne lidar, color air photographs and ground measurements, *Water Resour. Res.*, 47, doi:10.1029/2010WR10319, 2011b.  
 Birth, G. S. and Mcvey, G. R.: Measuring the colour of growing turf with a reflectance spectrometer, *Agronomy Journal*, 60(86), 640–643, 1968.  
 Blanch, S. J., Ganf, G. G., and Walker, K. F.: Tolerance of riverine plants to flooding and exposure indicated by water regime, *Regulated Rivers: Research and Management*, 15, 43–62, 1999.  
 680 Carbonneau, P.E., Piégay, H.: Fluvial Remote Sensing for Science and Management, Wiley-Blackwell, Chichester, 440pp., 2012.  
 Caruso, B. S., Pithie, C., and Edmondson, L.: Invasive riparian vegetation response to flow regimes and flood pulses in a braided river floodplain, *J. Environ. Management*, 125, 156–168, 2013.  
 Corenblit, D., Tabacchi, E., Steiger, J., and Gurnell, A. M.: Reciprocal interactions and adjustments between fluvial landforms and

- vegetation dynamics in river corridors: A review of complementary approaches, *Earth Sci. Rev.*, 84(1-2), 56–86, 2007.
- Crouzy, B., Edmaier, K., Pasquale, N., and Perona, P.: Impact of floods on the statistical distribution of riverbed vegetation, *Geomorphology*, 202, 51–58, 2013.
- Decamps, H.: The renewal of floodplain forests along rivers: a landscape perspective, *Verh. Int. Verein. Limnol.*, 26, 35–59, 1996.
- Dunford R, Michel K, Gagnage M, Piégay H, and Trémelo M-L: Potential and constraints of Unmanned Aerial Vehicle technology for the characterization of Mediterranean riparian forest, *International Journal of Remote Sensing*, 30(19), 4915–4935, doi:10.1080/01431160903023025, 2009.
- Eckert, S. and Engesser, M.: Assessing vegetation cover and biomass in restored erosion areas in Iceland using SPOT satellite data, *Appl. Geography*, 40, 179–190, 2013.
- Edmaier, K., Burlando, P., and Perona, P.: Mechanisms of vegetation uprooting by flow in alluvial non-cohesive sediment, *Hydrol. Earth Syst. Sci.*, 15, 1615–1627, 2011.
- Friedman, J. M. and Auble, G. T.: Mortality of riparian box elder from sediment mobilization and extended inundation, *Regulated Rivers: Research and Management*, 15, 463–476, 1999.
- Gitelson, A. A., Kaufman, Y. J., and Merzlyak, M. N.: Use of a green channel in remote sensing of global vegetation from EOS-MODIS, *Remote Sensing of Environment*, 58(3), 289–298, 1996.
- Glenn, E. P., Huete, A. R., Nagler, P. L., and Nelson, S. G.: Relationship between remotely-sensed vegetation indices, canopy attributes and plant physiological processes: what vegetation indices can and cannot tell us about the landscape. *Sensors*, 8(4), 2136–2160, 2008.
- Glenz, C., Schlaepfer, R., Iorgulescu, I., and Kienast, F.: Flooding tolerance of Central European tree and shrub species, *Forest Ecology and Management*, 235(1–3), doi:10.1016/j.foreco.2006.05.065, 2006.
- Gregory, S. V., Swanson, F. J., McKee, W. A., and Cummins, K. W.: An ecosystem perspective of riparian zones, *BioScience*, 41, 540–551, 1991.
- Gurnell, A. M. and Petts, G.: Trees as riparian engineers: The Tagliamento River, Italy, *Earth Surf. Process. Landforms*, 31(12), 1558–1574, 2006.
- Gurnell, A. M. and Petts, G.: Hydrology and ecology of river systems, in *Treatise on Water Science*, edited by Peter Wilderer, Elsevier, Oxford, 237–269, ISBN 9780444531995, 2011.
- Gurnell, A. M., Bertoldi, W., and Corenblit, D.: Changing river channels: The roles of hydrological processes, plants and pioneer fluvial landforms in humid temperate, mixed load, gravel bed rivers, *Earth Science Reviews*, 11(1–2), 129–141, 2012.
- Hatfield, J. L.: Plant-water interactions, in *Plants for Environmental Studies*, edited by Wuncheng, W., Gorsuch, J. W., Hughes, J., CRC Press, 81–100, 1997.
- Huete, A. R.: A soil adjusted vegetation index (SAVI), *Remote Sensing of Environment*, 25(3), 295–309, 1988.
- Jackson, R. D., and Huete, A. R.: Interpreting vegetation indices, *Preventive Veterinary Medicine*, 11(3), 185–200, 1991.
- Jacobson, R. B.: Riverine Habitat Dynamics, In *Treatise on Geomorphology*, edited by John F. Shroder, Academic Press, San Diego, 6–19, ISBN 9780080885223, 2013.
- Johansen, K., Phinn, S., and Witte, C.: Mapping of riparian zone attributes using discrete return LiDAR, QuickBird and SPOT-5 imagery: Assessing accuracy and costs, *Remote Sensing of Environment*, 114(11), 2679–2691, 2010.
- Kozłowski, T.T. and Pallardy, S.G., 2002.: Acclimation and adaptive responses of woody plants to environmental stresses. *Botanical Review*, 68, 270–334.
- Latterell, J. J., Scott Bechtold, J., O’Keefe, T. C., Pelt, R., and Naiman, R. J.: Dynamic patch mosaics and channel movement in an unconfined river valley of the Olympic Mountains, *Freshwater Biology*, 51(3), 523–544, 2006.
- Loheide, S. P. and Booth, E. G.: Effects of changing channel morphology on vegetation, groundwater, and soil moisture regimes in groundwater-dependent ecosystems, *Geomorphology*, 126(3–4), 364–376, 2011.
- Meier, C. I. and Hauer, F. R.: Strong effect of coarse surface layer on moisture within gravel bars: Results from an outdoor experiment, *Water Resour. Res.*, 46, W05507, 2010.
- Merritt, D. M., Scott, M. L., Poff, L. N., Auble, G. T., and Lytle, D. A.: Theory, methods and tools for determining environmental flows for riparian vegetation: riparian vegetation-flow response guilds, *Freshwater Biology*, 55(1), 206–225, 2010.
- Mizunuma, T., Koyanagi, T., Mencuccini, M., Nasahara, K. N., Wingate, L., and Grace, J.: The comparison of several colour indices for the photographic recording of canopy phenology of *Fagus crenata* Blume in eastern Japan. *Plant Ecology & Diversity*, 4(1), 67–77, doi:10.1080/17550874.2011.563759, 2011.
- Molnar, P., Favre, V., Perona, P., Burlando, P., Randin, C., and Ruf, W.: Floodplain forest dynamics in a hydrologically altered mountain river, *Peckiana*, 5, 17–24, 2008.
- Morgan, J. L., Gergel, S. E., and Coops, N. C.: Aerial Photography: A Rapidly Evolving Tool for Ecological Management. *BioScience*, 60(1), 47–59, doi:10.1525/bio.2010.60.1.9, 2010.
- Mulla, D. J.: Twenty five years of remote sensing in precision agriculture: Key advances and remaining knowledge gaps, *Biosystems Engineering*, 114(4), 358–371, 2012.
- Nagai, S., Saitoh, T.M., Koayashi, H., Ishihara, M., Suzuki, R., Motohka, T., Nasahara, K.N., and Muraoka, H.: In situ examination of the relationship between various vegetation indices and canopy phenology in an evergreen coniferous forest, Japan, *Int. J. of Remote sensing*, 33(19), 6202–6214, 2012.
- Nilsson, C. and Berggren, K.: Alterations of Riparian Ecosystems Caused by River Regulation, *BioScience*, 50(9), 783–792, 2000.
- Ortiz, B. V., Thomson, S. J., Huang, Y., Reddy, K. N., and Ding, W.: Determination of differences in crop injury from aerial application of glyphosate using vegetation indices, *Computers and Electronics in Agriculture*, 77(2), 204–213, 2011.
- Parsons, M. and Thoms, M. C.: Patterns of vegetation greenness during flood, rain and dry resource states in a large, unconfined floodplain landscape., *J. Arid Environ.*, 88, 24–38, 2013.
- Pasquale, N., Perona, P., Francis, R., and Burlando, P.: Effects of streamflow variability on the vertical root density distribution of willow cutting experiments, *Ecological Eng.*, 40, 167–172, 2012.
- Pasquale, N., Perona, P., Wombacher, A., and Burlando, P.: Hydrodynamic model calibration from pattern recognition of non-orthorectified terrestrial photographs, *Computers & Geosciences*, 62, 160–167, 2014.
- Perona, P., Molnar, P., Savina, M., and Burlando, P.: An observation-based stochastic model for sediment and vegetation dynamics in the floodplain of an Alpine braided river, *Water Resour. Res.*, 45, doi:10.1029/2008WR007550, 2009a.

- 815 Perona, P., Camporeale, C., Perucca, E., Savina, M., Molnar, P.,  
Burlando, P., and Ridolfi, L.: Modelling river and riparian vege-  
tation interactions and related importance for sustainable ecosys- 875  
tem management, *Aquat. Sci.*, 71(3), 266–278, 2009b.
- Perona, P., Molnar, P., Crouzy, B., Perucca, E., Jiang, Z., McLel-  
land, S., and Gurnell, A. M.: Biomass selection by floods and  
820 related timescales: Part 1. Experimental observations, *Advances  
in Water Resour.*, 39, 85–96, 2012. 880
- Pringle, C. M., Naiman, R. J., and Bretschko, G.: Patch dynamics  
in lotic systems: The stream as a mosaic, *J. North American Ben-  
thological Soc.*, 7(4), 503–524, 1988.
- 825 Richardson, A.D., Jenkins, J.P., Braswell, B.H., Hollinger, D.Y.,  
Ollinger, C.V., and Smith, M.-L.: Use of digital webcam images 885  
to track spring green-up in a deciduous broadleaf forest, *Oecolo-  
gia*, 152, 323–334, 2007.
- Richardson, A. D., Braswell, B. H., Hollinger, D. Y., Jenkins, J.  
830 P., and Ollinger, S. V.: Near-surface remote sensing of spatial  
and temporal variation in canopy phenology. *Ecological Appli- 890  
cations*, 19(6), 1417–1428. doi:10.1890/08-2022.1, 2009.
- Rouse, J. W. Jr., Haas, R. H., Deering, D. W., Schell, J. A., and  
Harlan, J. C.: Monitoring the vernal advancement and retrograda-  
835 tion (green wave effect) of natural vegetation, Greenbelt, MD:  
NASA/GSFC Type III Final Report, 1974.
- Qi, J., Chebouni, A., Huete, A. R., Kerr, Y. H., and Sorooshian,  
S.: A modified soil adjusted vegetation index, *Remote Sensing of  
Environment*, 48(2), 119–126, 1994.
- 840 Sims, D.A. and Gamon, J.A.: Relationships between leaf pigment  
content and spectral reflectance across a wide range of species,  
leaf structures and development stages, *Remote Sensing of Envi-  
ron.*, 81, 337–354, 2002.
- Sims, D. A. and Gamon, J. A.: Estimation of vegetation water con-  
845 tent and photosynthetic tissue area from spectral reflectance : a  
comparison of indices based on liquid water and chlorophyll ab-  
sorption features, *Remote Sensing of Environment*, 84(4), 526–  
537, 2003.
- Sripada, R. P., Schmidt, J. P., Dellinger, A. E., and Beegle, D. B.:  
850 Evaluating Multiple Indices from a Canopy Reflectance Sensor  
to Estimate Corn N Requirements, *Agronomy Journal*, 100(6),  
1553–1561, 2008.
- Tal, M. and Paola, C.: Effects of vegetation on channel morphody-  
namics: results and insights from laboratory experiments, *Earth  
855 Surf. Process. Landforms*, 35(9), 1014–1028, 2010.
- Tockner, K. and Stanford, J. A.: Riverine flood plains: present  
state and future trends, *Env. Conservation*, 29(3), 308–330,  
doi:10.1017/S037689290200022X, 2002.
- Tockner, K., Bunn, S. E., Gordon, C., Naiman, R. J., Quinn, G.  
860 P., Standord, J. A., and Polunin, N. V. C.: Flood plains: criti-  
cally threatened ecosystems, in: Aquatic ecosystems: trends and  
global prospects, Polunin, N. V., Edinburgh, Cambridge Univer-  
sity Press, 45–61, 2008.
- Toda, Y., Ikeda, S., Kumagai, K., and Asano, T.: Effects of flood  
865 flow on flood plain soil and riparian vegetation in a gravel river,  
*J. Hydraulic. Eng.*, 131, 950–960, 2005.
- Verrelst, J., Schaepman, M. E., Koetz, B., and Kneubühler, M.:  
Angular sensitivity analysis of vegetation indices derived from  
CHRIS/PROBA data, *Remote Sensing of Environment*, 112(5),  
870 2341–2353, 2008.
- Viña, A., Gitelson, A. A., Nguy-Robertson, A. L., and Peng, Y.:  
Comparison of different vegetation indices for the remote as-  
sessment of green leaf area index of crops, *Remote Sensing of  
Environment*, 115(12), 3468–3478, 2011.
- Vincini, M., Frazzi, E., and D’Alessio, P.: A broad-band leaf chloro-  
phyll vegetation index at the canopy scale, *Precision Agriculture*,  
9(5), 303–319, 2008.
- Welber, M., Bertoldi, W., and Tubino, M.: The response of braided  
planform configuration to flow variations, bed reworking and  
vegetation: the case of the Tagliamento River, Italy, *Earth Surf.  
Process. Landforms*, 37(5), 572–582, 2012.
- Zarco-Tejada, P.J., Berni, J.A.J., Suarez, L., Sepulcre-Canto, G.,  
Morales, F., and Miller, J.R.: Imaging chlorophyll fluorescence  
with an airborne narrow-band multispectral camera for vegeta-  
tion stress detection, *Remote Sensing of Environ.*, 113, 1262–  
1275, 2009.
- Zhang, C. and Kovacs, J. M.: The application of small unmanned  
aerial systems for precision agriculture: a review. *Precision  
Agriculture*, 13(6), 693–712, doi:10.1007/s11119-012-9274-5,  
2012.

**Table 1.** Overview of the vegetation indices (VIs) used in this study. NIR, R, and G stand for the spectral reflectance in the near-infrared, visible red and visible green frequencies.  $L$  is a scaling constant, usually assigned the value 0.5.

	Vegetation Index	Formula	Reference
RVI	Red VI	$\text{NIR}/\text{R}$	Birth and Mcvey, 1968
GRVI	Green Ratio VI	$\text{NIR}/\text{G}$	Sripada et al., 2008
NDVI	Normalized Difference VI	$(\text{NIR} - \text{R})/(\text{NIR} + \text{R})$	Rouse et al., 1974
GNDVI	Green Normalized Difference VI	$(\text{NIR} - \text{G})/(\text{NIR} + \text{G})$	Gitelson et al., 1996
SAVI	Soil Adjusted VI	$(1 + L)(\text{NIR} - \text{R})/(\text{NIR} + \text{R} + L)$	Huete, 1988
GSAVI	Green Soil Adjusted VI	$(1 + L)(\text{NIR} - \text{G})/(\text{NIR} + \text{G} + L)$	Sripada et al., 2008
CVI	Chlorophyll VI	$\text{NIR} \cdot \text{R}/\text{G}^2$	Vincini et al., 2008

**Table 2.** Analysed floods in this study in the period 2008–2011. The return period of flood peaks is estimated from data for the period 1982–2011 at Bignasco (Source: Meteoswiss and FOEN).

Flood Date	No. of images before/after	Peak <sup>2</sup> $\text{m}^3\text{s}^{-1}$	Return period yrs
28.5.2008	2/4	192	1.4
6.6.2009	7/6	254	1.7
17.7.2009	6/7	272	1.9
12.6.2010	4/2	301	2.2
13.7.2011	5/6	598	20.1

**Table 3.** Index of Disagreement ID in % of the total number of pixels where two VIs disagree on the direction of vegetation change, i.e. vegetation damage or enhancement.

	NDVI	GNDVI	RVI	GRVI	SAVI	GSAVI	CVI	Mean
NDVI		17.9	0.7	17.9	10.1	22.1	31.9	16.8
GNDVI	17.9		17.9	0.7	20.4	12.3	17.3	14.4
RVI	0.7	17.9		17.8	10.3	22.2	31.9	16.8
GRVI	17.9	0.7	17.8		20.5	12.5	17.4	14.5
SAVI	10.1	20.4	10.3	20.5		18.3	32.2	18.6
GSAVI	22.1	12.3	22.2	12.5	18.3		18.9	17.7
CVI	31.9	17.3	31.9	17.4	32.2	18.9		24.9

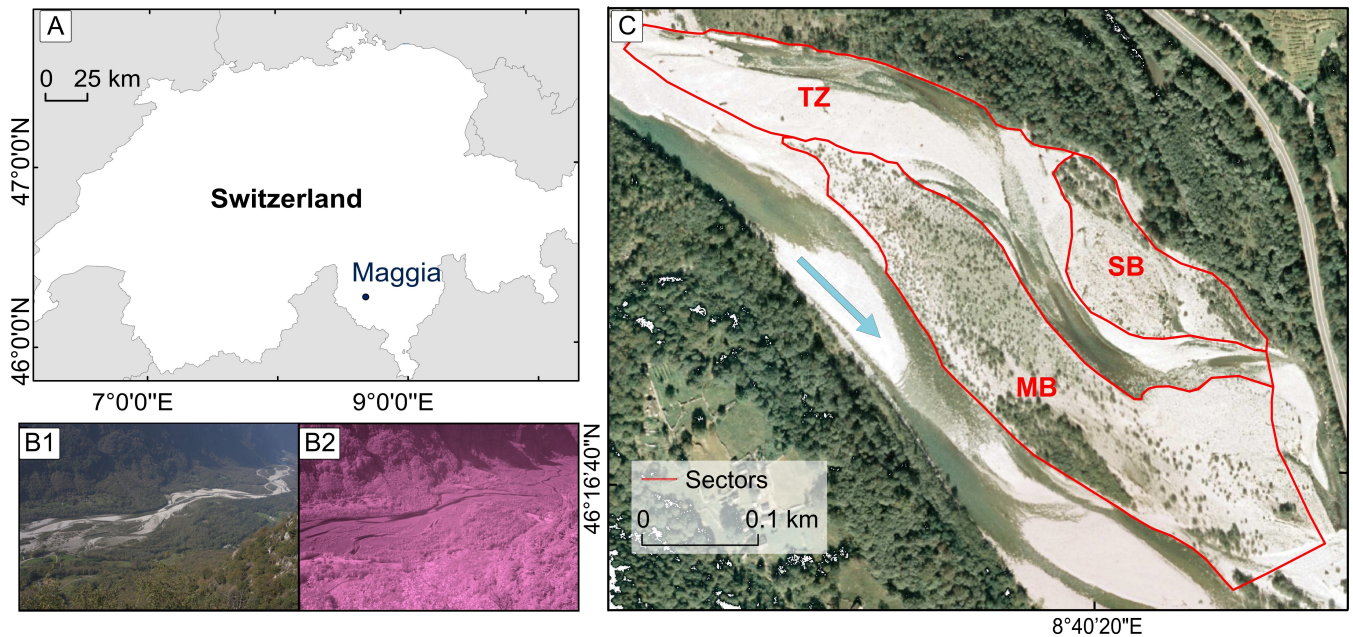


**Fig. 1.** A) Study reach location within Switzerland, B) Maggia valley view from the cameras (VIS top and IR bottom), C) Study reach subdivided into three units: main alluvial bar (MB), secondary alluvial bar (SB), transitional zone (TZ); blue arrow depicts the direction of flow.



**Fig. 2.** Typical vegetation composition of the Maggia floodplain. From left: gravel bar detail with small herbaceous plants and taller 1-3 yr salix saplings; 2-3 m tall salix trees which range up to 5-6 yrs in age; and tall salix, poplar and alder trees which have been found to be up to 20 yrs in age. Flood debris is visible at the stems of larger trees.

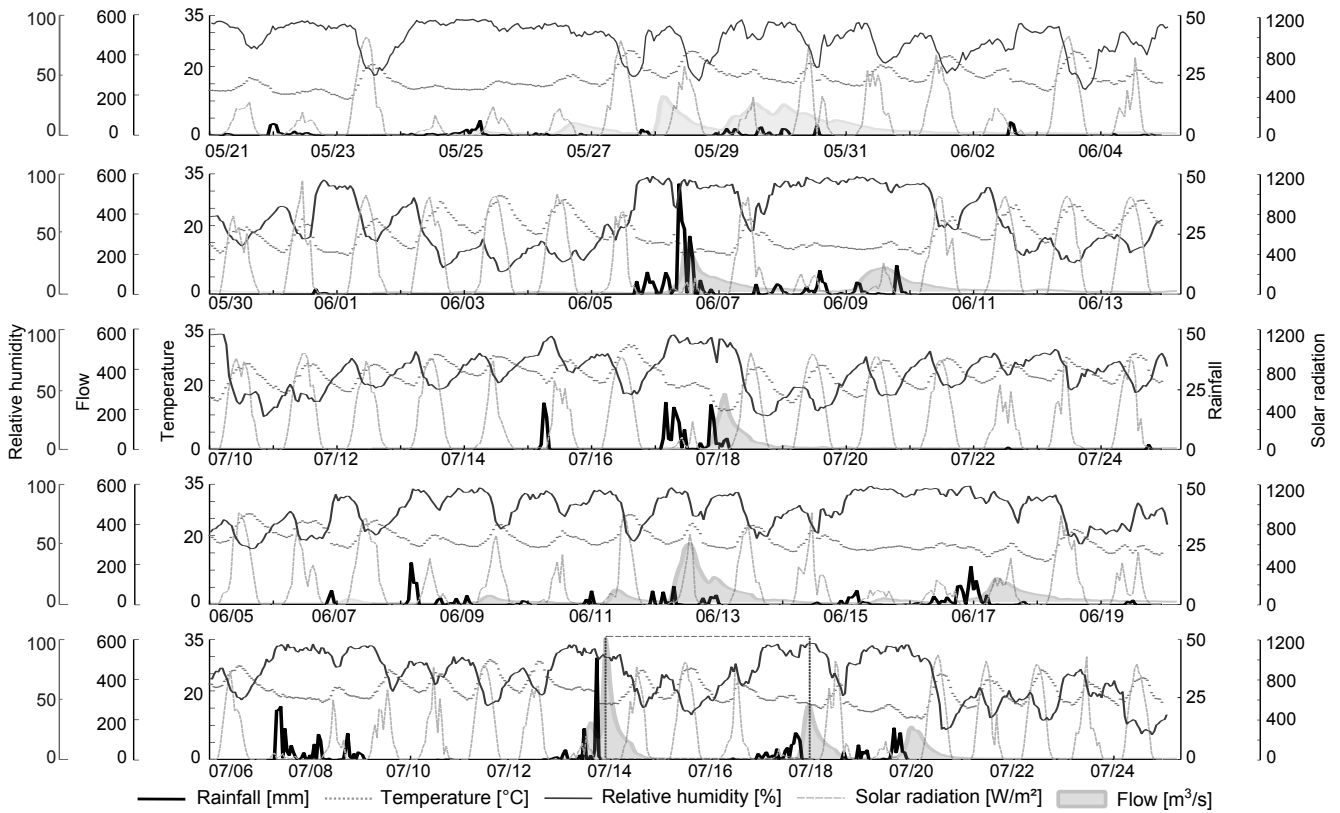


**Fig. 3.** Meteorological and hydrological conditions seven days before and after each flood. Floods are arranged according to Table 2, from top (2008) to bottom (2011).



**Fig. 4.** Spatial detail of the upstream section of the study reach with predicted vegetation scour (non-transparent/transparent red color) after flood in July 2011 shown together with the actual distribution of vegetation on the surface: A) full view on the study reach with estimated vegetation scour, B) detail on pre-flood distribution of vegetation, image from 11/7/2011, C) detail on post-flood distribution of vegetation, image from 22/7/2011.

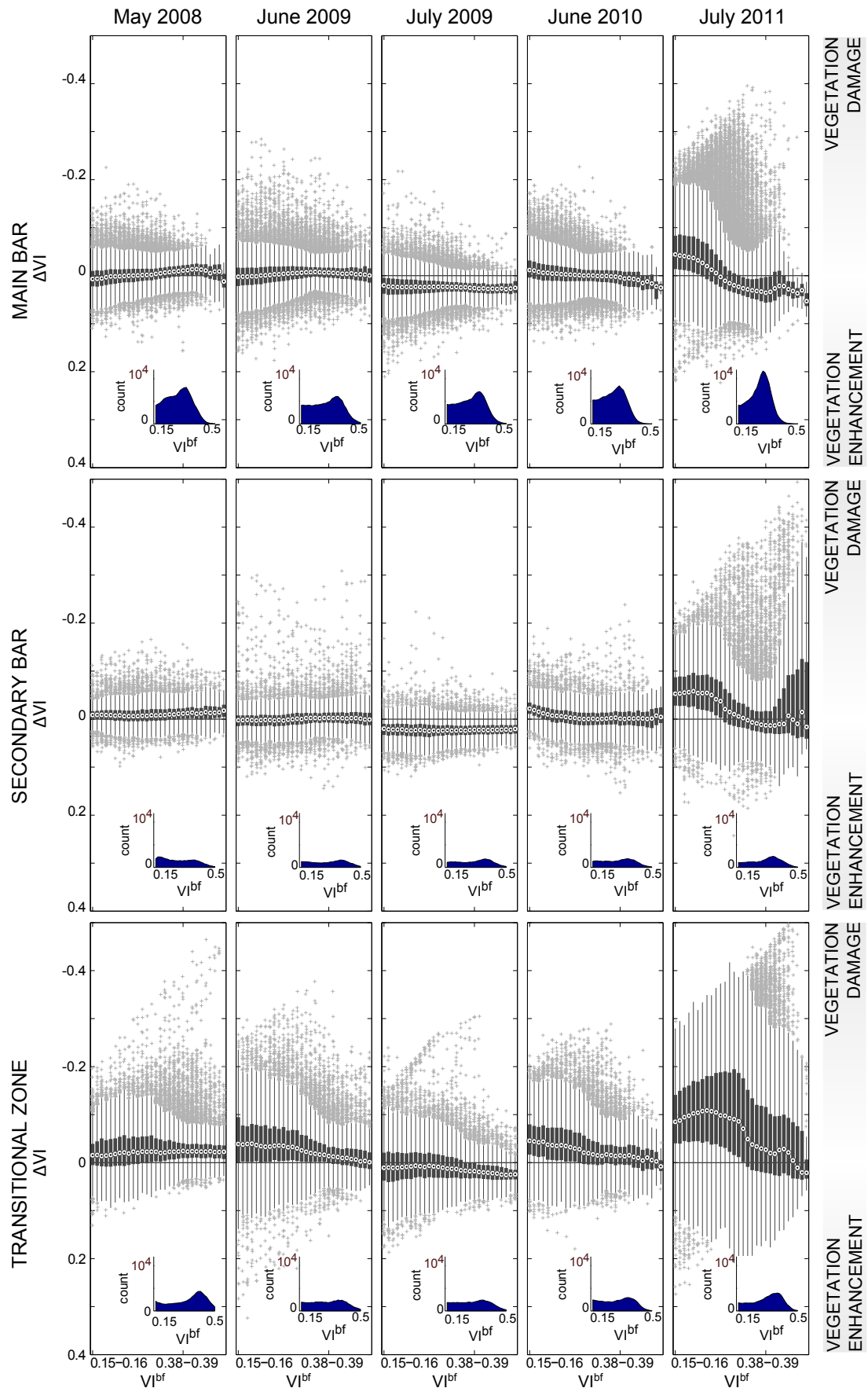


**Fig. 5.** Box plots for vegetation response  $\Delta VI$  with respect to the VI recorded before the flood.  $\Delta VI < 0$  indicates vegetation damage and  $\Delta VI > 0$  vegetation enhancement. Points are drawn as outliers if they are larger than  $q3 + 1.5(q3 - q1)$  or smaller than  $q1 - 1.5(q3 - q1)$ , where  $q1$  and  $q3$  are the 25th and 75th percentiles, respectively.

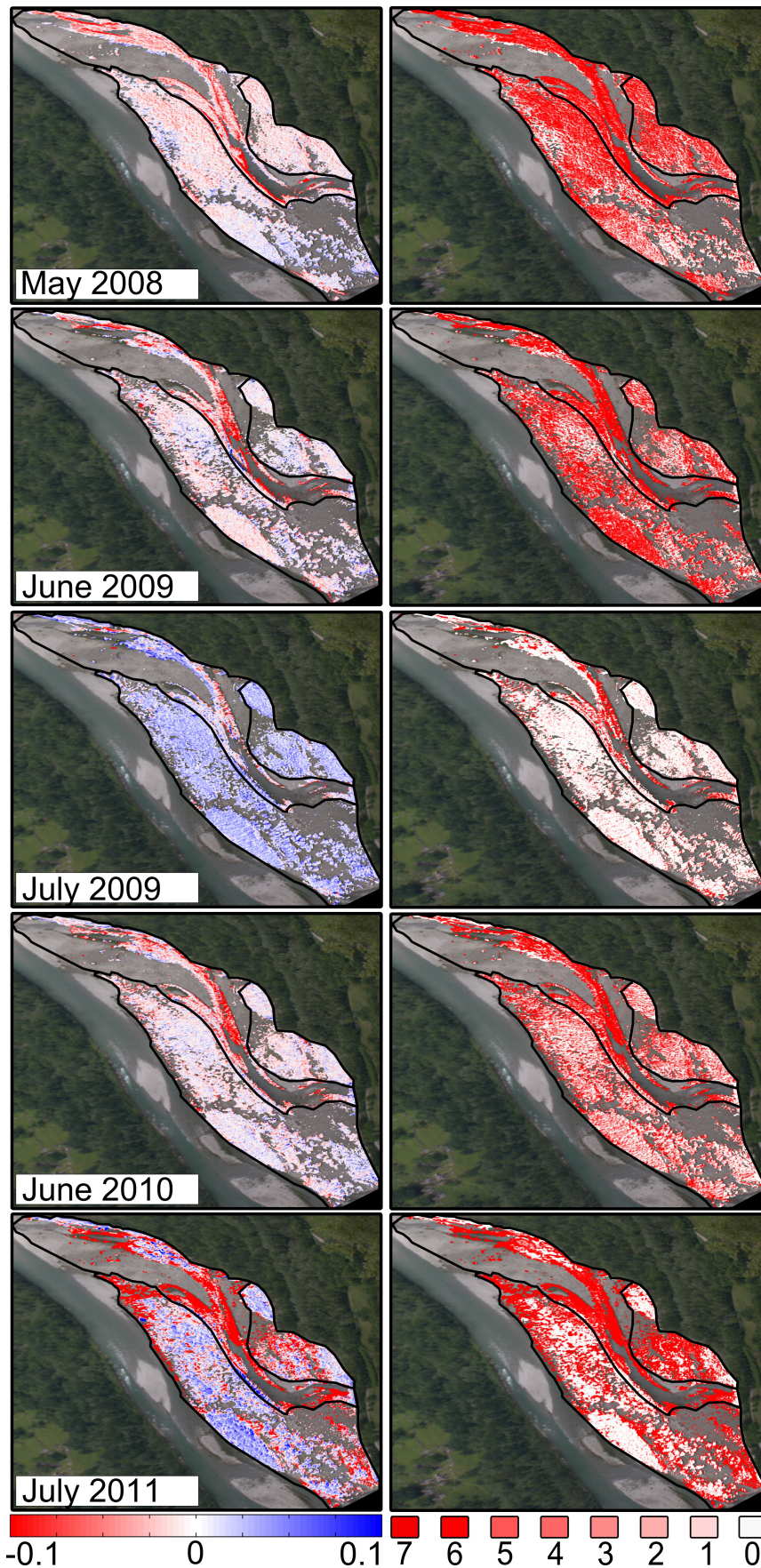


**Fig. 6.** Left column: Spatial distribution of vegetation response  $\Delta VI$  to each flood.  $\Delta VI < 0$  indicates vegetation damage and  $\Delta VI > 0$  vegetation enhancement. Right column: Number of VIs indicating vegetation damage for each flood. Base image: camera image from 01-06-2008.